Raman Spectroscopic Study on the Solvation of *N*,*N*-Dimethyl-*p*-nitroaniline in Room-Temperature Ionic Liquids

Yoshifumi Kimura,*,† Takuya Hamamoto,‡ and Masahide Terazima§

Division of Research Initiatives, International Innovation Center, Kyoto University, Kyoto 606-8501, Japan, Department of Chemistry, Faculty of Science, Kyoto University, Kyoto 606-8502, Japan, and Department of Chemistry, Graduate School of Science, Kyoto University, Kyoto 606-8502, Japan

Received: March 13, 2007; In Final Form: May 24, 2007

Electronic absorption spectra and Raman spectra of *N*,*N*-dimethyl-*p*-nitroaniline (DMPNA) have been measured in various fluids from the gaseous-like conditions in supercritical fluids (SCFs) to highly polar room-temperature ionic liquids (RTILs). We found that the S_0-S_1 absorption band center of DMPNA in RTILs is mostly determined by the molar concentrations of ions. On the other hand, the bandwidth of the absorption spectrum does not follow the expectation from a simple dielectric continuum model. Especially in SCFs, the bandwidth of the absorption spectrum decreases with increasing solvent density, suggesting that the intramolecular reorganization energy is a decreasing function of the solvent density. The Raman shift of the NO_2 stretching mode has been proven to be a good indicator of the solvent polarity; i.e., the vibrational frequency of the NO_2 stretching mode changes from 1340 cm^{-1} in mostly nonpolar solvent such as ethane to 1300 cm^{-1} in water. The linear relationship between the absorption band center and the vibrational frequency of the NO_2 mode, which was observed for conventional liquids in a previous paper (Fujisawa, T.; Terazima, M.; Kimura, Y. *J. Chem. Phys.* **2006**, *124*, 184503), holds almost well for all fluids including SCFs and RTILs. On the other hand, the vibrational bandwidth does not show a simple relationship with the absorption band center. The vibrational bandwidths in RTILs are generally larger in comparison with those in conventional liquids with similar polarity scales. Among the RTILs we investigated, the vibrational bandwidth loosely correlates with the molecular size of the anion. A similar dependence on the anion size is also observed for the bandwidth of the absorption spectrum. We have also investigated the excitation wavelength dependence of the Raman shift of the NO_2 stretching mode in RTILs. The extent of the dependence on the excitation wavelength in all fluids is well correlated with the vibrational bandwidth.

1. Introduction

Solvatochromic shift of a molecule in solution has been widely used to characterize the properties of solvents. Various kinds of probe molecules have been used to investigate solvent properties, such as the polarity, the hydrogen-bonding ability, and so on.[1] The solvatochromic shift occurs due to the energy shifts of the electronic ground and excited states induced by the solvent. Along with this solvent-induced change of the electronic state, the vibrational spectra of the solvatochromic molecules are frequently altered. In fact, there are many studies on the Raman spectra of the solvatochromic molecules, especially in relation to the intramolecular electron transfer reaction process.[2−8] For example, the vibrational spectrum of betaine (2,6-diphenyl-4-(2,4,6-triphenyl-*N*-pyridino) phenolate), which is one of the most famous solvatochromic molecules for the $E_T(30)$ scale, has been studied by several researchers. The relationship between the band shift and the vibrational structure change has been discussed in detail.[8] However, most of the solvents used in these studies were limited to conventional liquid solvents, and Raman spectroscopic study of these solvatochromic dyes in new classes of solvents such as room-temperature ionic liquids (RTILs) is quite rare.

RTILs, which are composed of cations and anions, belong to a new class of solvent fluids.[9] Their unique compositions attract much attention from chemists, and research in this field is now rapidly expanding. Solvatochromic shifts in RTILs have been studied extensively since an earlier stage of the research.[10−19] The most widely studied solvatochromic property is $E_T(30)$. The values of $E_T(30)$ for typical RTILs such as 1,3-dialkylimidazolium salts are between 0.4 and 0.65, which are close to a typical value in polar solvents such as dimethyl sulfoxide (DMSO) and alcohols.[10,15] Znamenskiy and Kobrak performed molecular dynamics simulations on the solvatochromic shift of betaine in 1-butyl-3-methylimidazolium hexafluorophosphate,[20] and discussed the effect of solute−solvent specific interaction and the screening effect of the long-range interactions. Kamlet−Taft solvatochromic parameters such as the dipolarity/polarizability parameter (π^*), the hydrogen-bond-acceptor basicities (β), and the hydrogen-bond-donor acidities (α) have also been investigated for several classes of RTILs.[10] It has been reported that the values of π^* are generally close to 1, indicating the large dipolarity/polarizability of RTILs. The values of α and β are strongly dependent on the cations and anions, ranging from nearly 0 to 1.

Although studies on the vibrational spectra are expected to give us detailed insights into solvation in RTILs, approaches from the vibrational spectrum of the solute molecule in RTILs have been rare. In our previous paper, we have studied the

* Corresponding author. Telephone: +81-75-753-4024. Fax: +81-75-753-4000. E-mail: ykimura@iic.kyoto-u.ac.jp.
† International Innovation Center.
‡ Faculty of Science.
§ Graduate School of Science.

10.1021/jp072020u CCC: $37.00
Published on Web 07/10/2007

SCHEME 1: Molecular Structures and Resonance Forms of PB and DMPNA

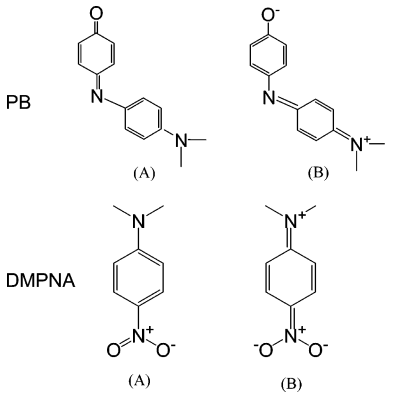

vibrational spectra of phenol blue (PB) in RTILs.[21] PB is a typical solvatochromic dye whose solvatochromic shifts have been studied by various authors.[22−30] The electronic states of the ground and excited states of PB are approximately written by the resonance forms between A and B in Scheme 1. The neutral form (A) dominantly contributes to the ground state, and the charge-separated state to the excited state. According to the resonance Raman study in conventional liquids and supercritical fluids (SCFs),[23] it was found that the vibrational frequencies of the C═N and C═O stretching modes, which are the characteristic modes related to the charge transfer, show a good linear correlation with the absorption band center, indicating the correlation between the vibrational frequency and the electronic transition energy. Further, the vibrational bandwidth, or the fluctuation of the vibrational frequency, is correlated with the solvent reorganization energy, or the fluctuation of the electronic transition energy. It was also found that the Raman shift of the C═N stretching mode is dependent on the wavelength of the Raman excitation under the resonant condition as a result of these correlations.[24−26] In the study on RTILs, we found that the linear relationship between the absorption band center and the vibrational frequencies of C═N and C═O stretching modes holds well in RTILs as is observed in conventional liquids and SCFs.[21] On the other hand, the magnitude of the solvent fluctuation in RTILs shows a different dependence on the solvent polarity from that in conventional liquids, which was discussed in terms of the specific interaction in RTILs.[21]

In this paper, we will present studies on the Raman spectrum of *N*,*N*-dimethyl-*p*-nitroaniline (DMPNA) (see Scheme 1) and the excitation wavelength dependence of the Raman Stokes shift of the NO_2 stretching mode in various kinds of RTILs. DMPNA is also a typical solvatochromic molecule, and Kamlet−Taft solvatochromic parameters have been determined by the absorption spectra of related compounds such as *p*-nitroaniline (PNA), *N*,*N*-diethyl-*p*-nitroaniline (DEPNA), and *p*-nitroanisole.[31−35] The electronic states of DMPNA are also approximately described by the superposition of the resonant forms like PB (see Scheme 1). Due to this nature of the charge transfer transition between the ground and excited states, the absorption peak of DMPNA is occasionally used to estimate the π^* value in the replacement of *p*-nitroanisole.[35] While the vibrational spectra of PNA and DEPNA have also been studied extensively using Raman spectroscopy,[4,36,37] DMPNA has been little investigated. In our previous paper,[38] we have reported detailed studies of the Raman Stokes shifts of DMPNA at various excitation wavelengths in conventional liquid solvents. We found that the Raman Stokes shift of the NO_2 vibrational mode is strongly dependent on the solvent: the vibrational frequency becomes lower with increasing solvent polarity in accordance with the solvatochromic shift. Furthermore, we have also found that the Raman shift of the NO_2 stretching mode is dependent on the excitation wavelength in polar solvents, which is similar to the case of PB;[24−26] the vibrational frequency of the NO_2 stretching mode once decreases from the nonresonant condition (647 nm excitation) to the resonant condition (452 nm excitation), and then increases again to the blue edge of the absorption (355 nm) in methanol. The phenomenon was interpreted by solvation state selective excitation as in the case of PB;[26] i.e., by choosing a particular wavelength for excitation, a solute molecule with a specific vibrational frequency is selectively excited from an inhomogeneously broadened absorption spectrum due to the coupling between fluctuations in the electronic transition energy and the vibrational frequency. The study on the Raman spectra in RTILs is expected to reveal the characteristic fluctuation of the dipolar solute molecule in RTILs.

In the following section, the experimental methods will be described in detail. For comparison with the previous study of PB, experiments not only in RTILs but also in SCFs have also been performed. By using SCFs, we can survey a region extended to the gaseous region, in which the property will be a reference state to see the solvent effect. Here we have chosen three typical SCFs, ethane (C_2H_6), carbon dioxide (CO_2), and trifluoromethane (CHF_3), whose critical temperatures are close to the room temperature, while the types of intermolecular interactions are quite different from one another. In section 3, the experimental results are presented together with the discussion. First, the absorption band center and shape are discussed in detail. Then the Raman spectra of the NO_2 stretching mode in various fluids are presented. The peaks and bandwidths are discussed in relation to the polarity scale determined by the absorption band center. Finally, the excitation wavelength dependence in RTILs is presented.

2. Experimental Section

2.1. Materials. DMPNA was purchased from Lancaster and used after recrystallization from ethanol before use. Conventional organic solvents (cyclohexane (C_6H_{12}), benzene (C_6H_6), dimethyl sulfoxide (DMSO), methanol (MeOH), dimethylformamide (DMF): spectroscopic grade) were purchased from Nacalai Tesque, and used as received. Gases of ethane (C_2H_6, Sumitomo Seika, >99.0%), carbon dioxide (CO_2, Kyoto Teisan, >99.9%), and trifluoromethane (CHF_3, Daikin, >99.999%) were used as received. RTILs used in this study are listed in Table 1 (the abbreviations of the names of RTILs are given in Table 1). [AEIm]Br, [ABIm]Br, [EMIm][BF_4], [BMIm][BF_4], [AEIm][BF_4], [ABIm][BF_4], [BMIm][NTf_2], [$N_{1,1,1,3}$][NTf_2], and [$Pp_{1,3}$][NTf_2] were purchased from Kanto Kagaku. [EMIm][$EtOSO_3$] was kindly supplied by Solvent Innovation. [BM_2Im][BF_4], [BPy][BF_4], and [HPy][BF_4] were purchased from Acros. [$P_{6,6,6,14}$][NTf_2] was purchased from Merck. [EMIm][$(HF)_{2.3}F$] was kindly supplied by Prof. R. Hagiwara (Kyoto University). [BMIm][PF_6] was synthesized and purified according to ref 39.

All measurements for conventional solvents and RTILs were performed at 25.0 °C. Since the melting point of [AEIm]Br was reported to be 55.4 °C,[40] the solution was in the supercooled state. The concentrations of DMPNA were typically less than 20 mM, and the solutions of RTILs were filtered by using a membrane filter (50 μm) to remove undissolved solute. The solutions were evacuated using a vacuum line ($<1.3 \times 10^{-1}$ Pa) more than 2 h before each experiment. The contents of water

TABLE 1: List of Ionic Liquids Used for the Measurements and Parameters Obtained from the Absorption and Raman Spectra at 488 nm Excitation

no.	name[j]	ρ (g cm^{-3})	C (mol dm^{-3})	ω_a[a] (cm^{-1})	$\Delta\omega_a$[a] (cm^{-1})	polarity scale[a]	π^*	ν_{NO_2}[a] (cm^{-1})	$\Delta\nu_{NO_2}$[a] (cm^{-1})
1	[AEIm]Br	1.341[a]	6.18	24 760	3730	1.13		1299.1	31.7
2	[ABIm]Br	*b*		24 950	3730	1.08		1300.6	32.3
3	[EMIm][$(HF)_{2.3}$F]	1.130[c]	6.42	25 240	3890	1.00	1.026[a]	1305.0	28.6
4	[EMIm][$EtOSO_3$]	1.237[a]	5.24	25 030	3730	1.05		1304.8	25.5
5	[EMIm][BF_4]	1.280[a]	6.47	25 210	3900	1.00		1305.3	29.0
6	[BMIm][BF_4]	1.208[d]	5.33	25 270	3830	0.99	1.047,[h] 1.04[i]	1305.5	29.1
7	[BM_2Im][BF_4]	1.096[a]	4.57	25 200	3770	1.01	1.083[h]	1303.1	28.9
8	[AEIm][BF_4]	1.231[a]	5.50	25 180	3870	1.01		1304.8	30.3
9	[ABIm][BF_4]	1.168[a]	4.63	25 260	3830	0.99		1304.4	28.7
10	[BPy][BF_4]	1.220[e]	5.47	25 290	3810	0.98		1304.1	28.6
11	[HPy][BF_4]	1.154[a]	4.60	25 350	3830	0.97		1305.1	30.6
12	[BMIm][PF_6]	1.373[d]	4.82	25 310	3880	0.98	1.032,[h] 1.02[i]	1304.8	30.9
13	[BMIm][NTf_2]	1.429[d]	3.43	25 540	3970	0.92	0.984,[h] 0.964[i]	1306.3	30.0
14	[$N_{1,1,1,3}$][NTf_2]	1.440[f]	3.77	25 640	4040	0.89	0.970[i]	1306.3	31.8
15	[$Pp_{1,3}$][NTf_2]	1.410[a]	3.34	25 630	4010	0.89		1305.6	31.5
16	[$P_{6,6,6,14}$][NTf_2]	1.066[g]	1.40	25 820	3850	0.84		1308.0	28.4

[a] This work. Polarity scale is given by $[\omega_a - \omega_a(C_6H_{12})]/[\omega_a(DMSO) - \omega_a(C_6H_{12})]$. [b] The solution was too viscous for the density to be measured by the density meter of the vibrating tube oscillator. [c] Reference 48. [d] Reference 10. [e] Reference 47. [f] Reference 49. [g] Reference 50. [h] Reference 11. [i] Reference 46. [j] AEIm, 1-allyl-3-ethylimidazolium; ABIm, 1-allyl-3-butylimidazolium; EMIm, 1-ethyl-3-methylimidazolium; BMIm, 1-butyl-3-methylimidazolium; BM_2Im, 1-butyl-2,3-dimethylimidazolium; BPy, 1-butylpyridinium; HPy, 1-hexylpyridinium; $N_{1,1,1,3}$, *N*,*N*,*N*-trimethyl-*N*-propylammonium; $Pp_{1,3}$, *N*-methyl-*N*-propylpiperidinium; $P_{6,6,6,14}$, trihexyl(tetradecyl)phosphonium; NTf_2, bis(trifluoromethanesulfonly)imide; $EtOSO_3$, ethyl sulfate.

in RTILs were examined by Karl Fischer titration (MKC-610-DT, Kyoto Electronics Manufacturing Co. Ltd.) after the Raman measurement. The hydrophobicity of RTILs is mostly determined by the species of anion.[9] Therefore, we checked the water contents for typical RTILs with different species of anion. Typical water contents (w/w) of [BMIm][NTf_2] and [$N_{1,1,1,3}$]-[NTf_2] were 100 and 250 ppm, respectively, and those of [BMIm][BF_4] and [EMIm][BF_4] were 200 and 500 ppm. In the cases of very hydrophilic RTILs such as [EMIm][$EtOSO_3$] and [AEIm]Br the water contents were 0.2%. The effect of the water impurity on the experimental result will be discussed in section 3.2.

2.2. Apparatus. Raman spectra of DMPNA were measured mostly at a 90° scattering geometry using a 64 cm monochromator (Jobin Yvon, T6400, a 1800 lines/mm grating) equipped with a CCD detector (Princeton Instrument, Spec-10:400BRXTE) and suitable edge filters. An Ar ion laser (Coherent, Enterprise; 363.8 nm, 457.9 nm, 488.0 nm), a Kr ion laser (Omnichrome, 643-MRDN-AO1; 568.2 nm, 647.1 nm), a pulsed Nd:YAG laser (Continuum, Minilite, 355 nm, 15 Hz), and a pulsed dye laser (Continuum, ND6000, 420 nm) pumped by a Nd:YAG laser (Continuum, Surelite II-10, 355 nm, 10 Hz) were used as the excitation lasers. For the measurements in RTILs under the strongly resonant conditions (355 or 363 nm excitation), a backscattering geometry was employed for the detection. In RTILs, DMPNA showed degradation when it was excited at the resonant condition. Therefore, the measurements at 363 nm were performed by using a 1 cm quartz cell with continuous stirring of the sample solution using a magnetic stirrer. For the other experiments, the measurements were performed without any stirring of the solution. The Raman shift calibration was performed by the Raman spectra of C_6H_6 and C_6H_{12}. The spectrum sensitivity of the system was corrected by using the fluorescence spectra of reference samples (quinine, *m*-nitrodimethylaniline, 2-aminopyrizine).[41,42] The absorption spectra were measured using a UV−vis spectrometer (Shimazu UV-2400). The densities of RTILs were measured by a vibrating tube oscillator at 25.00 °C (Anton Paar, DMA4500).

For the measurements in SCFs, a high-pressure optical cell and a high-pressure system were used, the details of which are described elsewhere.[23,43,44] Briefly, a high-pressure optical cell equipped with four quartz windows was used for the Raman measurements at 90° scattering geometry. The temperature of the cell was regulated at 50.0 (±0.2) °C by flowing the thermostated water through the cell, and the pressure of the fluid was monitored by a strain gauge (Kyowa, PGM-500KH). The density of the solvent was calculated by empirical equations of state.[45] In the measurement, a measured amount of DMPNA was put in the cell, and the sample was dissolved by a magnetic stirrer inside the cell after the introduction of the high-pressure fluid from the reservoir. Measurements were generally performed successively from a lower pressure to a higher pressure.

3. Results and Discussion

3.1. Solvatochromic Shift of DMPNA. Figure 1 shows absorption spectra of DMPNA in (a) conventional liquids, (b) RTILs, and (c) SCFs at various pressures. The absorption peak position shows a very large shift from nearly 30 000 cm^{-1} in ethane at 6.29 MPa to 23 640 cm^{-1} in water. The peak positions in RTILs are close to that in DMSO as was reported for a similar kind of solvatochromic probe previously.[10] No concentration dependence of the absorption spectra was detected for the solutions of RTILs in our study. As is shown in the figure, not only the absorption peak position but also the absorption band shape is dependent on the solvent. Therefore, we tried to estimate the absorption band center (ω_a) by fitting the absorption band shape to a sum of log-normal functions as is described in the previous paper.[38,44] The absorption band center is defined as

$$\omega_a = \int \nu g(\nu)\, d\nu / \int g(\nu)\, d\nu \quad (1)$$

where

$$\epsilon(\nu) \propto \nu g(\nu) \quad (2)$$

Here $\epsilon(\nu)$ and $g(\nu)$ are the absorption coefficient and the absorption line shape function, respectively. The line shape function $g(\nu)$ in the fluid studied here was fit well by at most two components of log-normal functions as was described in the previous paper.[38] The uncertainty of the band center was estimated to be ±100 cm^{-1}.

TABLE 2: List of Conventional Liquids Used for the Measurements and Parameters Obtained from the Absorption and Raman Spectra at 488 nm Excitation

name[d]	ω_a/cm^{-1}	$\Delta\omega_a$/cm^{-1}	polarity scale[a]	π^* [b]	ν_{NO_2}/cm^{-1}	$\Delta\nu_{NO_2}$/cm^{-1}
C_6H_{12}	28 870	3840	0	0	1330.0	16.1
C_6H_6	26 960	3760	0.52	0.55	1321.2	19.6
BuOH	26 470	4440	0.66	0.48	1314.7	30.3
PrOH	26 390	4450	0.68	0.54	1314.3	30.6
EtOH	26 340	4480	0.69	0.54	1314.4	31.1
MeOH	26 080	4320	0.77	0.60	1312.4	31.1
ACN	25 970	3940	0.80	0.66	1313.0	22.2
DMF	25 630	3750	0.89	0.88	1308.5	22.9
DMSO	25 230[c]	3710[c]	1	1	1304.6[c]	30.2[c]
water	24 230	4460	1.28	1.09	1299.9	30.0

[a] Polarity scale is given by $[\omega_a - \omega_a(C_6H_{12})]/[\omega_a(DMSO) - \omega_a(C_6H_{12})]$. [b] Reference 1. [c] This work. [d] C_6H_{12}, cyclohexane; C_6H_6, benzene; BuOH, 1-butanol; PrOH, 1-propanol; EtOH, ethanol; MeOH, methanol; ACN, acetonitrile; DMF, dimethylformamide; DMSO, dimethyl sulfoxide. The results except for DMSO were taken from ref 38.

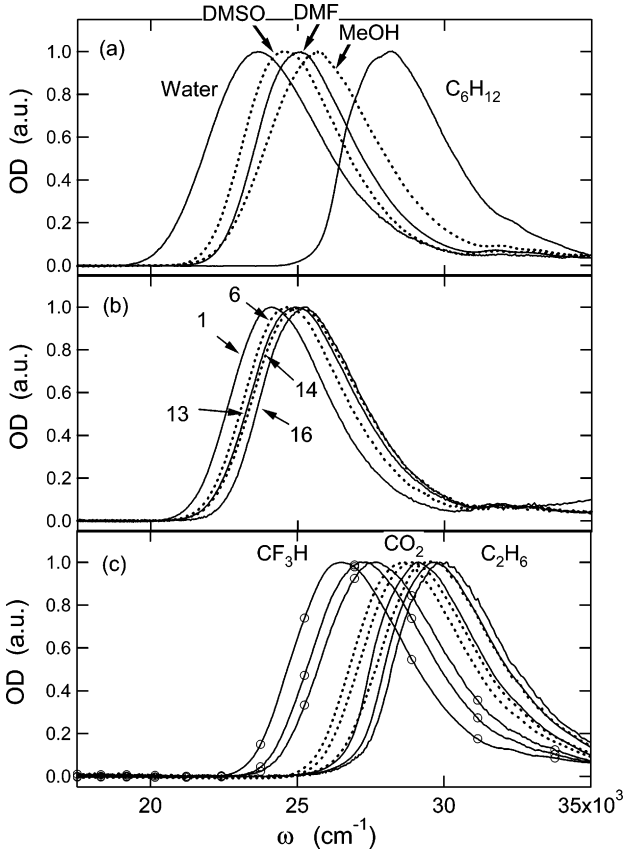

Figure 1. Absorption spectra of DMPNA in various fluids. (a) In conventional liquids at room temperature. From left to right: water, DMSO, DMF, MeOH, and C_6H_{12}. (b) In RTILs at 25.0 °C. The numbers in the figures are the substance indexes given in Table 1. From left to right: 1, 6, 13, 14, and 16. (c) In SCFs at 50.0 °C at various pressures. From left to right: CHF_3 (—⊖—) at 6.35, 8.71, and 29.01 MPa; CO_2 (- - -) at 8.92, 11.58, and 17.02 MPa; C_2H_6 (—) at 6.29, 7.29, and 26.87 MPa, respectively.

The polarity scales, which correspond to the traditional π^* values, were determined by the relative shift of ω_a from that in C_6H_{12} assuming that the polarity scale is 1 for DMSO and 0 for C_6H_{12}, respectively. The values of the polarity scale defined here in the conventional liquid solvents are close to the reported values of π^* (Table 2),[1] although our estimated values are slightly larger than the traditional π^* values. We consider that this difference is caused by the band shape changes due to the solvent: i.e., the Franck−Condon progression which is weakly observed in the nonpolar solvent is smeared out in the polar solvents, and the contribution of the higher energy region of the absorption spectrum becomes smaller.

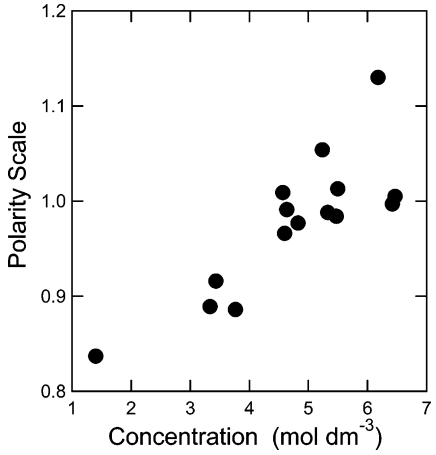

Figure 2. Molar concentration dependence of the polarity scale of DMPNA in RTILs at 25.0 °C.

As shown in Table 1, the polarity scales of RTILs are around 1, similar to the reported π^* values.[10,11,46] However, the detailed examination indicates that there is a variation of the polarity scales from the minimum value (0.84) of $[P_{6,6,6,14}][NTf_2]$ to the maximum value (1.13) of [AEIm]Br. The solvent species dependence of this value is similar to the reported values of π^* as is shown in Table 1. We believe the main factor that determines the spectrum shift of DMPNA is the ionic concentration. Figure 2 plots the polarity scale against the molar concentrations of RTILs which are calculated from density[10,47−50] and molecular weight. As is shown in the figure, there is a trend that the polarity scale increases with increasing the molar concentration of RTIL. This correlation is similar to the previous case of PB.[21] The molar concentration reflects the charge concentration within a unit volume of the solution. Therefore, it is reasonable that the solvatochromic shift due to the dipolarity/polarizability is related to this property.[51]

Figure 3 shows the relationship between the polarity scale and the full width at half-maximum (fwhm) of the absorption spectrum ($\Delta\omega_a$). As is shown in the previous paper,[38] no clear correlation was observed between ω_a and $\Delta\omega_a$ in conventional liquids. Generally speaking, $\Delta\omega_a$ is determined by two factors:[52] one is the solvent reorganization energy, which is directly related to the solvent polarity scale, and the other is the intramolecular vibrational reorganization energy, which is determined by the difference of the vibrational structure between the electronic ground and excited states. Theoretically, $\Delta\omega_a$ increases with increases of the solvent reorganization energy and the intramolecular vibrational reorganization energy. The apparent absence of the correlation between the polarity scale (or the solvent reorganization energy) and $\Delta\omega_a$ in the present

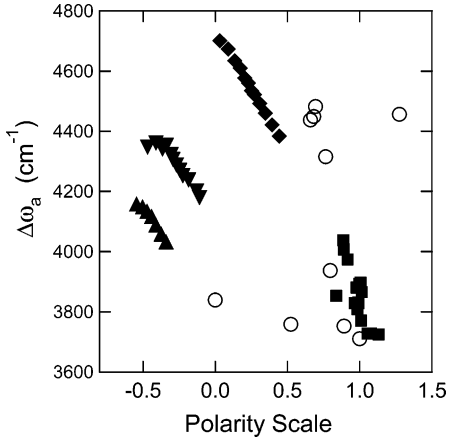

Figure 3. Correlation between the absorption bandwidth ($\Delta\omega_a$) and the polarity scale determined by the absorption band center (ω_a) in various fluids: (○) conventional liquids at RT, (■) RTILs at 25.0 °C, (▲) C_2H_6 ($\rho_r = 0.97-1.96$), (▼) CO_2 ($\rho_r = 0.49-1.89$), and (◆) CHF_3 ($\rho_r = 0.51-2.01$). The results for SCFs are at 50.0 °C.

case (Figure 3) means that the intramolecular reorganization energy, or the molecular structure of the solute, is expected to be strongly dependent on the solvent. This point is clearly seen in the density dependence of $\Delta\omega_a$ in SCFs. The values of the polarity scale of SCFs determined here are close to the π^* values of SCFs determined previously.[53,54] In SCFs, $\Delta\omega_a$ decreases with increasing solvent density, as is observed for PB.[23] If the solvent reorganization energy in the solvents dominates $\Delta\omega_a$, $\Delta\omega_a$ is expected to increase with increasing solvent density, since the solvent reorganization energy increases with an increase of the solvent density as is represented by the solvent density dependence of the polarity scale.[55] The decrease of $\Delta\omega_a$ indicates that the intramolecular reorganization energy, which is another factor to determine $\Delta\omega_a$, decreases with increasing solvent density. This means that the displacement of the intramolecular vibrational coordinate in the ground state compared with that in the excited state becomes smaller with increasing solvent density or, equivalently, polarity. This is reasonable considering that the contribution of the charge-separated state in the electronic ground state increases with increasing solvent polarity (see Scheme 1).

It is also to be noted that the lower density limits of both $\Delta\omega_a$ and the polarity scale in all SCFs should take the same values. Therefore, a very large density effect is expected in the lower density region especially for CHF_3 and CO_2; e.g., $\Delta\omega_a$ will decrease with decreasing solvent density in the lower density region. This complexity of the density dependence is due to the competitive effect of the intramolecular reorganization energy and solvent reorganization energy.

The values of $\Delta\omega_a$ in RTILs are similar to those of DMSO and DMF: rather smaller than those in the solvents which have hydrogen-bonding ability. It seems that $\Delta\omega_a$ becomes smaller with increasing polarity scale, and that $\Delta\omega_a$ is dependent on the anion rather than on the cation. These points will be discussed again in terms of the bandwidth of the Raman spectrum.

3.2. Raman Spectra of DMPNA. Figure 4 shows the Raman spectra of DMPNA in various RTILs obtained at 488 nm excitation. The very strong band around 1300 cm^{-1} was assigned to the NO_2 stretching mode.[38] For several RTILs (e.g., [BM_2Im]-[BF_4], [BPy][BF_4], [HPy][BF_4], and [ABIm]Br), weak fluorescence signals were detected, probably due to the contaminations. These background fluorescence signals together with the solvent signals were removed from the Raman spectra of the solution

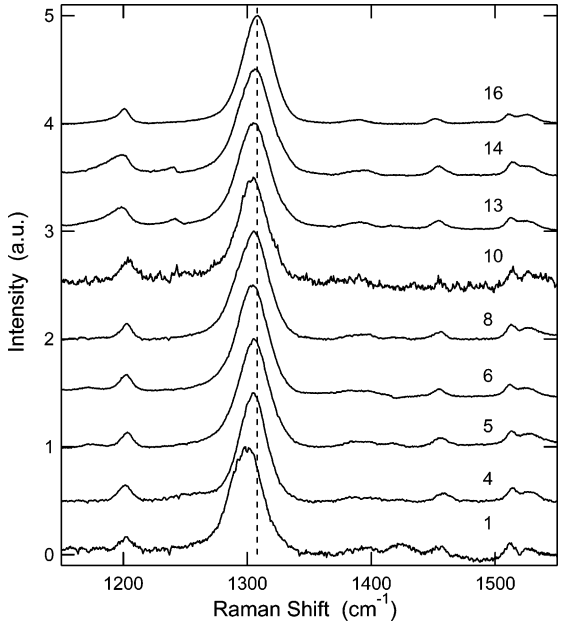

Figure 4. Raman spectra of DMPNA in various RTILs at 25.0 °C obtained by 488 nm excitation. The numbers in the figure are the substance indexes given in Table 1.

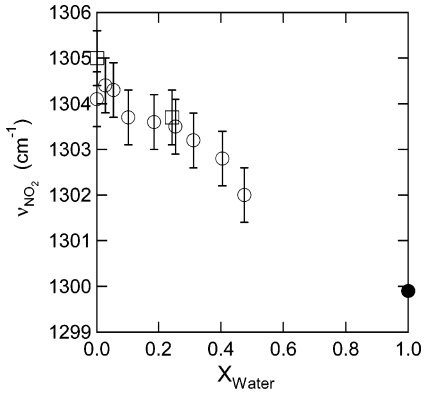

Figure 5. Effect of water concentration on the Raman shift of the NO_2 stretching mode in [BMIm][BF_4] (○) and [BMIm][NTf_2] (□). The result in pure water is also shown (●).

by subtracting the Raman spectra of the solvents. The Raman spectra in RTILs are quite similar to one another, although there are small differences in the peak positions and bandwidths of the NO_2 stretching mode depending on the cations and anions. The band shape of the NO_2 stretching mode is mostly approximated by a Gaussian function, although there is a slight asymmetry in the band shape: i.e., there is a tail in the smaller frequency region. Therefore we determined the fwhm of the vibrational band ($\Delta\nu_{NO_2}$) from the observed signal directly, and the peak position (ν_{NO_2}) was determined by the fitting to a Gaussian function around the peak position.

Before a detailed discussion on the Raman signal in RTILs, we examined the effect of the water contamination in RTILs on the Raman shift. Figure 5 shows how the Raman shift of the NO_2 stretching mode changes with the mole faction of water (X_{water}) in a hydrophilic RTIL ([BMIm][BF_4]) and a hydrophobic RTIL ([BMIm][NTf_2]). In the case of [BMIm][BF_4], we gradually added a measured amount of water to the solution of DMPNA, where the concentration of water in the original solution was determined by Karl Fischer titration. In the case of [BMIm][NTf_2], we compared two solutions: one was the dried solution and the other was the ionic liquid phase solution extracted after mixing with water. The water concentrations of

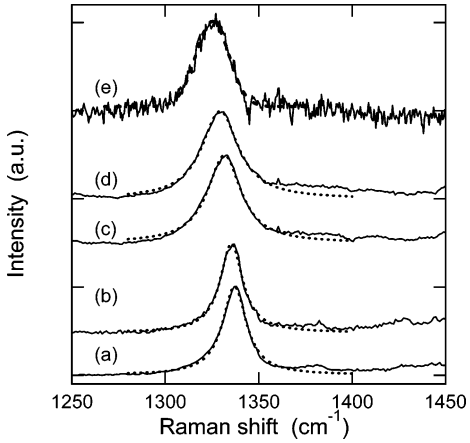

Figure 6. Raman spectra of DMPNA obtained at 355 nm excitation in supercritical fluids at 50.0 °C. In C_2H_6 at 7.30 (a) and 25.8 MPa (b), and in CHF_3 at 8.71 (c) and 29.0 MPa (d), respectively. The broken lines are the fit to the Lorentzian function. The result obtained at 488 nm excitation in CHF_3 at 29.0 MPa (e) is also shown.

these solutions were also determined by Karl Fischer titration. The concentration of water in the latter solution (13 700 ppm) was somewhat smaller than in the water-saturated solution (19 900 ppm).[56] As is shown in the figure, the vibrational frequency of the NO_2 stretching mode is almost linearly dependent on the mole fraction of water, although the dependence seems smaller near $X_{water} = 0$. Since most of our experiments were performed for RTILs with the contents of water typically less than 500 ppm (e.g., this value corresponds to 0.006 mole fraction in the case of [BMIm][BF_4]) and the experimental accuracy of the wavenumber at 488 nm excitation was within ± 0.6 cm^{-1}, the effect on the Raman shift by such a small amount of water can be ignored in the present study.

Figure 6 shows the Raman spectra around the region of the NO_2 stretching mode of DMPNA in C_2H_6 and CHF_3 at different pressures obtained at 355 nm excitation under the resonant condition. The solubilities of DMPNA in SCFs were not enough to measure the nonresonant Raman signal at 488 nm excitation with enough signal-to-noise ratio (S/N), except for the highest density of CHF_3 (the signal is also plotted in Figure 6). The solvent bands were subtracted from the spectra of the solution by comparing the Raman spectra obtained for the solvent fluids. In CO_2, we could not observe the Raman spectrum with enough S/N even under the resonant condition, probably because the degradation of DMPNA occurs in CO_2. The band in C_2H_6 was fit well by a Lorentzian function (the broken line in the figure), while the fitting to the Lorentzian function becomes somewhat worse in CHF_3. The spectra for the nonresonant condition was well fit by a Gaussian function, although the S/N ratio is much worse than those obtained under the resonant condition. The different vibrational line shape in C_2H_6 is probably because the inhomogeneity of the solvent environment in C_2H_6 is quite small and the Raman band shape is predominantly determined by the dephasing time.

Now we discuss the relation between the absorption spectra (polarity scales) and the vibrational frequency of the NO_2 stretching mode. As is shown in the previous paper,[38] there is a good linear correlation between the absorption band center (ω_a) and the NO_2 vibrational frequency (ν_{NO_2}) excited at 488 nm in conventional liquids. Figure 7a shows the same plot including these values in RTILs and in SCFs, although most of the values in SCFs were obtained at 355 nm excitation. Here the horizontal scale is the polarity scale, which is equivalent to ω_a. As is shown in the figure, the linear relation holds almost

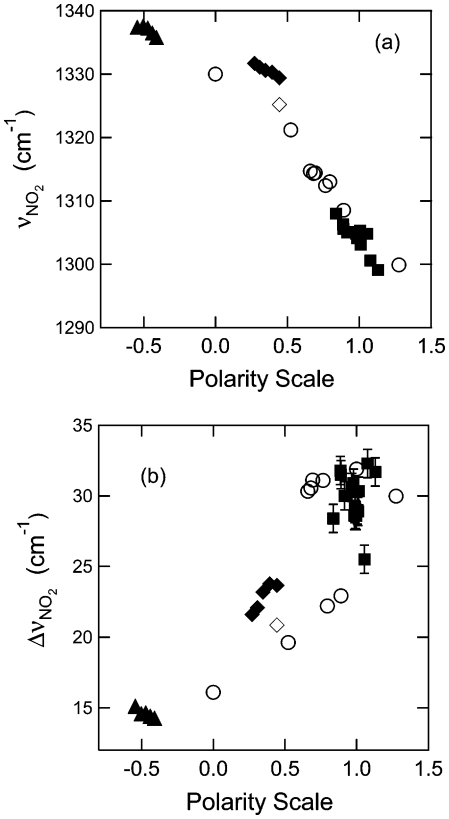

Figure 7. (a) Correlation between the vibrational frequency of the NO_2 stretching mode (ν_{NO_2}) and the polarity scale determined by the absorption band center (ω_a) in various fluids: (○) conventional liquids (488 nm excitation), (■) RTILs (488 nm excitation), (▲) C_2H_6 (355 nm excitation), (◆) CHF_3 (355 nm excitation), and (◇) CHF_3 (488 nm excitation), respectively. (b) Correlation between the vibrational bandwidth of the NO_2 stretching mode ($\Delta\nu_{NO_2}$) and the polarity scale. The meanings of the symbols are the same as in (a). Typical error bars are shown.

well including the data in ethane and RTILs. The clear deviation from the linear relation in the case of CHF_3 is mainly due to the difference of the wavelength of the excitation laser, because the Raman Stokes shift of the NO_2 stretching mode is dependent on the excitation wavelength in polar solvents as is reported previously[38] and will be shown later in this paper; i.e., in a polar solvent, the value of ν_{NO_2} obtained at 488 nm excitation is smaller than that obtained at 355 nm excitation. In fact, the value of ν_{NO_2} in CHF_3 for 488 nm excitation lies near the linear correlation. The existence of the excitation wavelength dependence of ν_{NO_2} indicates that the linear correlation between the polarity scale and ν_{NO_2} is dependent on the excitation wavelength of the Raman measurements. Similar plots of the NO_2 stretching vibrational frequencies obtained at different excitation wavelengths (355 and 647 nm) against the polarity scale are given in the Supporting Information. As is shown there, the linear correlation holds well for the other excitation wavelengths, although the slopes (the extent of the change of ν_{NO_2} against the polarity scale) are different.

The correlation between the polarity scale and ν_{NO_2} is understandable, if we consider that the vibrational mode of NO_2 is strongly coupled to the electronic state (see the resonance forms in Scheme 1). The solvent field which affects the charge distribution of the electronic states induces a similar change in ν_{NO_2}, irrespective of the source of the solute−solvent interaction, e.g., the ion−dipole interaction in RTILs, hydrogen bonding in alcoholic solvent, or dipole−dipole interaction. In this sense,

ν_{NO_2} is an indicator of the dipolarity/polarizability parameter as well as the absorption peak.

On the other hand, $\Delta\nu_{NO_2}$ seems more sensitive to the kinds of solute−solvent interactions. Figure 7b shows the relation between the polarity scale and $\Delta\nu_{NO_2}$. One may notice that $\Delta\nu_{NO_2}$ increases with increasing solvent polarity scale. This is understandable if a major origin of $\Delta\nu_{NO_2}$ is the local inhomogeneity around the solute molecule and this inhomogeneity increases with increasing solvent polarity scale.[52,55] However, if we see the details, there are some features of the interaction dependence of $\Delta\nu_{NO_2}$. First, $\Delta\nu_{NO_2}$ is large in hydrogen-bonded solvents, as mentioned in the previous paper.[38] This is considered to reflect the ability of a NO_2 group as a hydrogen-bonding acceptor. Second, $\Delta\nu_{NO_2}$ values in RTILs are generally larger than those in conventional solvent fluids with similar absorption shifts, and comparable to those in the hydrogen-bonding solvents. Before the detailed discussion on the dependence of the cations or anions, we will discuss this general trend of the larger fluctuation of the vibrational bandwidth.

As is shown in the previous paper,[38] $\Delta\nu_{NO_2}$ reflects the fluctuation of the solvent field responsible for the change in the dipole moment of the solute molecule; e.g., $\Delta\nu_{NO_2}$ was almost linearly correlated with the fluorescence Stokes shift of a dipolar molecule such as Coumarin 153 (C153).[57,58] Until now, a number of studies have been performed on the static and dynamic fluorescence Stokes shift in RTILs.[59−62] According to these studies, a significant part of the solvent fluctuation in RTILs comes from configuration or the correlated translational movement of cations and anions, and the relaxation process is quite slow which extends to over several nanoseconds. The large inhomogeneity of the vibrational frequency in the present case is also expected to reflect the configurational distributions of the cations and anions. In this sense, the dependence of $\Delta\nu_{NO_2}$ on the cations and anions is an interesting issue. As is seen in Table 1, $\Delta\nu_{NO_2}$ is loosely correlated with the size of the anion; i.e., the bandwidth is smallest in the ionic liquid with $[EtOSO_3]^-$ anion and generally increases in the order of molecular size of anions $[BF_4]^-$, $[PF_6]^-$, and $[NTf_2]^-$, although there are some exceptions. The bandwidths in RTILs with Br^- are the largest, while the molecular size is smallest among the anions used in this study. Considering that the NO_2 group is negatively charged, one may expect that the bandwidth is more sensitive to the cation. The observed correlation between $\Delta\nu_{NO_2}$ and the anion suggests the correlated motions between cation and anion, which has been mentioned in the study of dynamics fluorescence Stokes shift,[59−61] is also important in the fluctuation of solvation.

A quite similar dependence of $\Delta\nu_{NO_2}$ on the anion is also seen for $\Delta\omega_a$ in RTILs. As is shown in Table 1, $\Delta\omega_a$ is also classified loosely by the anion species in a similar manner with $\Delta\nu_{NO_2}$; i.e., the value of $\Delta\omega_a$ is larger in the RTIL with the larger value of $\Delta\nu_{NO_2}$. We consider that the change of $\Delta\omega_a$ within RTILs is due to the solvent fluctuation and that this correlation is due to the coupling between the electronic transition energy and the vibrational frequency as is shown in Figure 7a.

It should be mentioned here that RTIL with $[P_{6,6,6,14}]^+$ cation shows relatively a large deviation from the above-mentioned correlation; i.e., in $[P_{6,6,6,14}][NTf_2]$, the fluctuation is not so large as those in other RTILs of $[NTf_2]^-$ anion. The very large molecular size of the cation may be the reason for the difference. In the study of the solvation dynamics, the ionic liquids which have alkylphosphonium cations show dependences different from those other common ionic liquids used in this study.[61b] Maroncelli et al. indicated that the viscosity dependence of the solvation time of C153 in alkylphosphonium is different from those in other RTILs; i.e., the solvation time is slower in comparison with other RTILs with similar viscosities.[61b] This is ascribed to the larger molecular size of the alkylphosphonium cation. In the present case, due to the bulky structure of the alkylphosphonium cation, the ionic concentration of alkylphosphonium ionic liquid is much smaller than those of the other ones, which reduces the effect of the charge fluctuation on the vibrational frequency of the NO_2 mode.

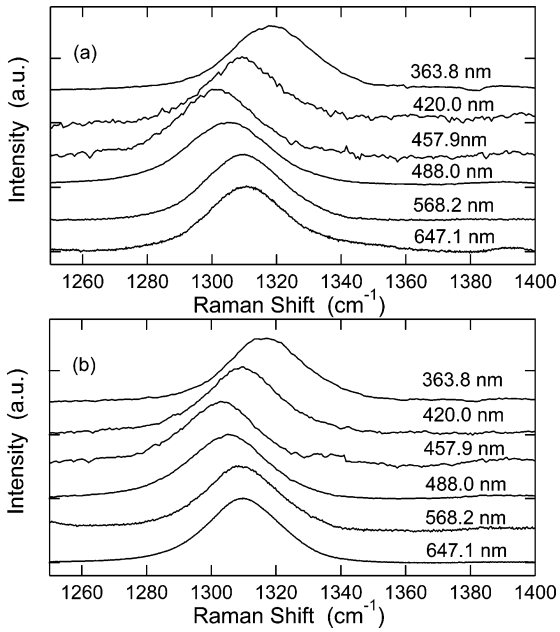

Figure 8. Raman spectra of DMPNA in RTILs obtained at various excitation wavelengths. (a) [BMIm][NTf_2] and (b) [EMIm][BF_4].

3.3. Excitation Wavelength Dependence of the Raman Stokes Shift of DMPNA. As was demonstrated in the previous paper,[38] ν_{NO_2} is dependent on the wavelength of the Raman excitation laser light under the resonant condition. The phenomenon was explained by the solvation state selective excitation;[25,26] i.e., the absorption spectrum of DMPNA in solution is broadened by the fluctuation of the surrounding solvent molecules. The molecule which shows the absorption in the blue edge of the spectrum is expected to have the higher ν_{NO_2}, because of the relationship between ω_0 and ν_{NO_2} in Figure 7a. By tuning the wavelength used for the Raman excitation, we can selectively probe the molecule with different solvent environments, which results in the excitation wavelength dependence of ν_{NO_2}.

Figure 8 shows typical examples of the excitation wavelength dependence of ν_{NO_2} in RTILs. The Raman spectra obtained here are quite similar to those observed in the case of MeOH.[38] Under the nonresonant condition (647 nm excitation), the band is almost symmetrical and centered around 1310 cm^{-1}. When the excitation wavelength shifts to the absorption red edge, ν_{NO_2} shifts to the lower frequency region, and takes the minimum value (1300 cm^{-1}) at the excitation around 458 nm. Then ν_{NO_2} shifts to the higher frequency again. The traces of ν_{NO_2} in several RTILs together with those in conventional liquids are shown in Figure 9. In all solvents except in water, the minimum values of ν_{NO_2} were around 22 000 cm^{-1}.

According to the theoretical model calculation,[26] the extent of the change of the Raman shift reflects the solvent fluctuation, if the vibrational dephasing time constant is shorter than the solvent relaxation time. In the case of RTILs, since the solvation time is reported to be generally extended to several nanoseconds

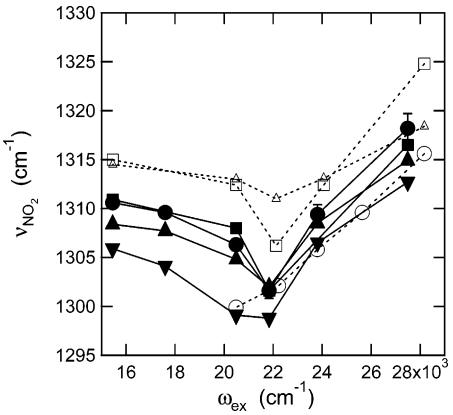

Figure 9. Excitation wavelength dependence of the Raman Stokes shift of the NO_2 stretching mode in various RTILs and conventional liquids. Typical errors are shown in the case of [BMIm][NTf_2]. (○) Water, (△) ACN, (□) MeOH, (●) [BMIm][NTf_2], (■) [$P_{6,6,6,14}$][NTf_2], (▲) [EMIm][$EtOSO_3$], and (▼) [AEIm]Br, respectively.

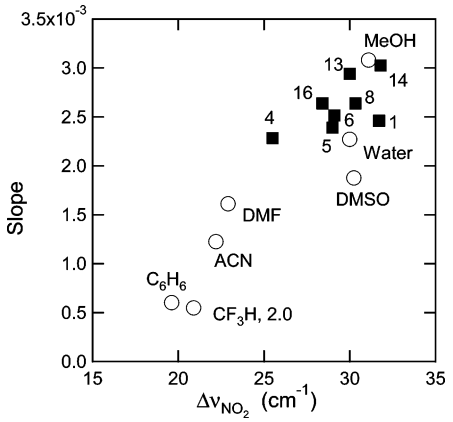

Figure 10. Correlation between the slope of the vibrational frequency against the excitation wavelength and the vibrational bandwidth of the NO_2 stretching mode.

from studies on the solvation dynamics, the vibrational dephasing time, which is usually on the order of picoseconds, should be much faster.[59−62] Therefore, the slope of the plot of ν_{NO_2} against the excitation wavelength can be a measure of the solvent fluctuation in RTILs.[26] Figure 10 shows the relationship between the slope of the excitation wavelength dependence and $\Delta\nu_{NO_2}$ obtained at 488 nm excitation. Here the slope was calculated by the change of the Raman shift from near the minimum value (at 457.9 or 452 nm excitation) to the maximum value (at 355 or 363.8 nm excitation). As is shown in the figure, there is a good linear correlation between them, indicating that the solvent fluctuation is a key to the observed phenomena. The magnitude of the slope in RTILs is dependent on the anion as observed for $\Delta\omega_a$; i.e., the slope becomes larger with increasing molecular size of the anion including the bromide anion. The resemblance of anion size dependence of the slope to $\Delta\omega_a$ supports the idea that the excitation wavelength dependence of the Raman shift results from the coupling between the fluctuations of the electronic transition energy and the vibrational frequency; i.e., a molecule with a certain value of ν_{NO_2} was selectively probed within an inhomogeneously broadened absorption spectrum ($\Delta\omega_a$) by choosing an excitation wavelength for the Raman detection.

It is also to be noted that the slope in RTILs decreases with increasing solvent polarity scale as in the case of $\Delta\omega_a$ (see the Supporting Information), while the slope increases with increasing solvent polarity scale in conventional liquids. The decrease of the slope with increasing solvent polarity in RTILs is also seen in the case of PB.[21] Generally, the solvent reorganization energy increases with an increase of the solvent polarity.[52,55] If the slope reflects the magnitude of the solvent fluctuation, the slope is expected to increase with an increase of the solvent polarity scale as is observed for conventional liquids. The result in RTILs contradicts this simple expectation. In the previous paper, we mentioned a possibility that the suppression of the solvent fluctuation occurs with stronger solvation by a small anion such as Cl^-. Here we also found the tendency of a decrease of the solvent fluctuation (or the slope) with decreasing the size of the anion and with increasing polarity scale. The anion size dependence is consistent with the polarity dependence, since the polarity scale tends to decrease with increasing anion size. The question is, what is the physical origin which reduces the fluctuation with decreasing anion size and/or with increasing the polarity scale of RTILs? At present, we do not have an answer for this question. Probably the bulky anion prevents the cation from taking the most favorable solvation structure around the solute, and induces the energy fluctuation of the solvation of cation. A detailed investigation by using simulations will be desirable in the future.

4. Conclusion

In this paper, we studied the S_0-S_1 absorption spectra and Raman spectra of DMPNA in fluids including nonpolar SCFs and various kinds of RTILs. From the absorption band centers (ω_a) we determined the dipolarity/polarizability of fluids. We found that the polarity scale of RTILs is mostly determined by the molar concentration of the fluids. The analysis of the bandwidth of the absorption spectrum ($\Delta\omega_a$) in SCFs suggests that the intramolecular reorganization energy decreases with increasing solvent density or polarity scale. In RTILs, $\Delta\omega_a$ was found to be mostly dependent on the molecular size of the anion (decreases with decreasing molecular size).

The Raman shift of the NO_2 stretching mode of DMPNA (ν_{NO_2}) obtained at 488.0 nm excitation was found to be almost linearly dependent on the solvent polarity scale, and this dependence is similar to that shown in the previous paper.[38] This reflects that ν_{NO_2} can be an indicator of the solvent polarity, and rather insensitive to the origin of the molecular interactions. On the other hand, the vibrational bandwidth of the NO_2 stretching mode ($\Delta\nu_{NO_2}$) did not show a simple relationship with the polarity scale of the solvent. $\Delta\nu_{NO_2}$ in RTILs is generally larger in comparison with the conventional liquids with similar ω_a. Within the RTILs, $\Delta\nu_{NO_2}$ was dependent mostly on the anion species as was observed in the case of $\Delta\omega_a$; i.e., $\Delta\nu_{NO_2}$ tended to increase with increasing molecular size of the anion within the RTILs studied here although there were some exceptions.

We have also investigated the excitation wavelength dependence of the Raman shift of the NO_2 stretching mode in RTILs in detail. The value of ν_{NO_2} was at a minimum for the excitation wavelength near 450 nm. We have evaluated the extent of the dependence by the change of the vibrational frequency from near 450 nm excitation to 355 or 363 nm excitation. The dependence on the excitation wavelength was well correlated with $\Delta\nu_{NO_2}$ and $\Delta\omega_a$, reflecting that this phenomenon derives from the correlation of the fluctuations between the electronic transition energy and vibrational frequency. The extent of the excitation energy dependence in RTILs tended to be suppressed with increasing polarity scale of the solvent or with decreasing molecular size of the anion. This is quite interesting considering that the NO_2 group is expected to be solvated by positively charged cations. Probably the correlated motions between the

cations and anions are important for the observed phenomena and should be investigated in more detail in the future by, e.g., molecular simulations.

Acknowledgment. We are grateful to Prof. R. Hagiwara (Kyoto University) for kindly supplying the synthesized ionic liquid [EMIm][$(HF)_{2.3}$F]. We are also grateful to Dr. Y. Yoshimura for the use of the density meter. We thank Mr. T. Fujisawa (Kyoto University) for the measurements in conventional liquids and Mr. M. Fukuda (Kyoto University) for some experiments on the solvatochromic shift of [EMIm][$(HF)_{2.3}$F]. This work is supported by Grants-in-Aid for Scientific Research from JSPS (Nos. 16350010 and 17073012).

Supporting Information Available: Tables of absorption spectral characteristics, and frequencies and bandwidths of NO_2 stretching mode in SCFs; figures giving the correlations between the polarity scale and the vibrational frequencies, and between the polarity scale and the excitation wavelength dependence. This material is available free of charge via the Internet at http://pubs.acs.org.

References and Notes

(1) Reichardt, C. *Solvents and Solvent Effects in Organic Chemistry*, 3rd ed.; Wiley-VCH: Weinheim, 2003.

(2) (a) Markel, F.; Ferris, N. S.; Gould, I. R.; Myers, A. B. *J. Am. Chem. Soc.* **1992**, *114*, 6208. (b) Kulinowski, K.; Gould, I. R.; Myers, A. B. *J. Phys. Chem.* **1995**, *99*, 9017. (c) Kulinowski, K.; Gould, I. R.; Ferris, N. S.; Myers, A. B. *J. Phys. Chem.* **1995**, *99*, 17715.

(3) Myers, A. B. *Chem. Phys.* **1994**, *180*, 215.

(4) Moran, A. M.; Kelley, A. M. *J. Chem. Phys.* **2001**, *115*, 912.

(5) Moran, A. M.; Egolf, D. S.; Blanchard-Desce, M.; Kelly, A. M. *J. Chem. Phys.* **2002**, *116*, 2542.

(6) Biswas, N.; Umapathy, S. *J. Chem. Phys.* **2003**, *118*, 5526.

(7) McHale, J. L. *Acc. Chem. Res.* **2001**, *34*, 265.

(8) (a) Zong, Y.; McHale, J. L. *J. Chem. Phys.* **1997**, *106*, 4963. (b) Zong, Y.; McHale, J. L. *J. Chem. Phys.* **1997**, *107*, 2920. (c) Zhao, X.; Burt, J. A.; McHale, J. L. *J. Chem. Phys.* **2004**, *121*, 11195.

(9) See, e.g.: *Ionic Liquids in Synthesis*; Welton, T., Ed.; Wiley-VCH: Weinheim, 2003; Hamaguchi, H.; Ozawa, R. *Adv. Phys. Chem.* **2005**, *131*, 85.

(10) Poole, C. F. *J. Chromatogr., A* **2004**, *1037*, 49.

(11) Crowhurst, L.; Mawdsley, P. R.; Perez-Arlandis, J. M.; Slater, P. A.; Welton, T. *Phys. Chem. Chem. Phys.* **2003**, *5*, 2790.

(12) Fletcher, K. A.; Storey, I. A.; Hendricks, A. E.; Pandey, S.; Pandey, S. *Green Chem.* **2001**, *3*, 210.

(13) Baker, S. N.; Baker, G. A.; Bright, F. V. *Green Chem.* **2002**, *4*, 165.

(14) Dzyuba, S. V.; Bartsch, R. A. *Tetrahedron Lett.* **2002**, *43*, 4657.

(15) Reichardt, C. *Green Chem.* **2005**, *7*, 339.

(16) Muldoon, M. J.; Gordon, C. M.; Dunkin, I. R. *J. Chem. Soc., Perkin Trans. 2* **2001**, 433.

(17) Wasserscheid, P.; Gordon, C. M.; Hilgers, C.; Muldoon, M. J.; Dunkin, I. R. *Chem. Commun.* **2001**, 1186.

(18) Carmichael, A. J.; Seddon, K. R. *J. Phys. Org. Chem.* **2000**, *13*, 591.

(19) Fredlake, C. P.; Muldoon, M. J.; Aki, S, N. V. K.; Welton, T.; Brennecke, J. F. *Phys. Chem. Chem. Phys.* **2004**, *6*, 3280.

(20) Znamenskiy, V.; Kobrak, M. N. *J. Phys. Chem. B* **2004**, *108*, 1072.

(21) Fujisawa, T.; Fukuda, M.; Terazima, M.; Kimura, Y. *J. Phys. Chem. A* **2006**, *110*, 6164.

(22) Figueras, J. *J. Am. Chem. Soc.* **1971**, *93*, 3255.

(23) Yamaguchi, T.; Kimura, Y.; Hirota, N., *J. Phys. Chem. A* **1997**, *101*, 9050.

(24) Yamaguchi, T.; Kimura, Y.; Hirota, N. *J. Chem. Phys.* **1997**, *107*, 4436.

(25) Yamaguchi, T.; Kimura, Y.; Hirota, N. *J. Chem. Phys.* **1998**, *109*, 9075.

(26) Yamaguchi, T.; Kimura, Y.; Hirota, N. *J. Chem. Phys.* **1998**, *109*, 9084.

(27) Kimura, Y.; Yamaguchi, T.; Hirota, N. *Phys. Chem. Chem. Phys.* **2000**, *2*, 1415.

(28) Morley, J. O.; Fitton, A. L. *J. Phys. Chem. A* **1999**, *103*, 11442.

(29) Nagasawa, Y.; Watanabe, A.; Ando, Y.; Okada, T. *J. Mol. Liq.* **2001**, *90*, 295.

(30) Chen, J.; Shen, D.; Wu, W.; Han, B.; Wang, B.; Sun, D. *J. Chem. Phys.* **2005**, *122*, 204508.

(31) Utley, J. H. P. *J. Chem. Soc.* **1963**, 3252.

(32) Kamlet, M. J.; Minesinger, R. R.; Kayser, E. G.; Aldridge, M. H.; Eastes, J. W. *J. Org. Chem.* **1971**, *36*, 3852.

(33) Kamlet, M. J.; Kyser, E. G.; Easter, J. W.; Gilligan, W. H. *J. Am. Chem. Soc.* **1973**, *95*, 377.

(34) Kamlet, M. J.; Taft, R. W. *J. Am. Chem. Soc.* **1976**, *98*, 377.

(35) Laurence, C.; Nicolet, P.; Dalati, M. T.; Abboud, J.-L. M.; Notario, R. *J. Phys. Chem.* **1994**, *98*, 5807.

(36) Schmid, E. D.; Moscchallski, M.; Peticolas, W. L. *J. Phys. Chem.* **1986**, *90*, 2340.

(37) (a) Mohanalingam, K.; Yokoyama, D.; Kato, C.; Hamaguchi, H. *Bull. Chem. Soc. Jpn.* **1999**, *72*, 389. (b) Mohanalingam, K.; Hamaguchi, H. *Chem. Lett.* **1997**, 537. (c) Mohanalingam, K.; Hamaguchi, H. *Chem. Lett.* **1997**, 157.

(38) Fujisawa, T.; Terazima, M.; Kimura, Y. *J. Chem. Phys.* **2006**, *124*, 184503.

(39) (a) Chen, J.; Shen, D.; Wu, W.; Han, B.; Wang, B.; Sun, D. *J. Chem. Phys.* **2005**, *122*, 204508. (b) Huddleston, J. G.; Wilauer, H. D.; Swatloski, R. P.; Visser, A. E.; Rogers, R. D. *Chem. Commun.* **1998**, *16*, 1765. (c) Holbrey, J. D.; Seddon, K. R. *J. Chem. Soc., Dalton Trans.* **1999**, 2133.

(40) Mizumo, T.; Maruwanta, E.; Matsumi, N.; Ohno, H. *Chem. Lett.* **2004**, *33*, 1360.

(41) Lipper, E.; Nägele, W.; Seibold-Blankenstein, I.; Staiger, U.; Vos, W. *Z. Anal. Chem.* **1959**, *170*, 1.

(42) Melhuish, W. H. *Appl. Opt.* **1975**, *14*, 26.

(43) Kimura, Y.; Yoshimura, Y. *J. Chem. Phys.* **1992**, *96*, 3085.

(44) Kimura, Y.; Hirota, N. *J. Chem. Phys.* **1999**, *111*, 4169.

(45) (a) Ethane: Younglove, B. A.; Ely, J. F. *J. Phys. Chem. Ref. Data* **1987**, *16*, 577. (b) Carbon dioxide: Span, R.; Wagner, W. *J. Phys. Chem. Ref. Data* **1996**, *25*, 1509. (c) Trifluoromethane: Rubio, R. G.; Zolloweg, J. A.; Streett, W. B. *Ber. Bunsen-Ges. Phys. Chem.* **1989**, *93*, 791.

(46) Tokuda, H.; Tsuzuki, S.; Susan, Md. A. B. H.; Hayamizu, K.; Watanabe, M. *J. Phys. Chem. B* **2006**, *110*, 19593.

(47) Noda, A.; Hayamizu, K.; Watanabe, M. *J. Phys. Chem. B* **2001**, *105*, 4603

(48) Hagiwara, R.; Matsumoto, K.; Tsuda, T.; Ito, Y.; Matsumoto, H.; Momota, K. *J. Electrochem. Soc.* **2003**, *150*, D195.

(49) Matsumoto, H.; Yanagida, M.; Tanimoto, K.; Nomura, M.; Kitagawa, Y.; Miyazaki, Y. *Chem. Lett.* **2000**, 922.

(50) Esperança, J. M. S. S.; Guedes, H. J. R.; Blesic, M.; Rebelo, L. P. N. *J. Chem. Eng. Data* **2006**, *51*, 237.

(51) It is noteworthy here that the polarity of an ionic liquid composed of specific anion [EMIm][$(HF)_{2.3}$F] was determined here. The polarity scale (1.0) of this ionic liquid is quite normal, as is that of ordinary ionic liquids. We also evaluated the π^* and β values by the traditional way and found that $\pi^* = 1.026$ and $\beta = 0.48$. The value of π^* is similar to the polarity scale determined here, and the value of β is close to those for ionic liquids with nitrate anion. The value of β is relatively larger than those for ionic liquids with $[BF_4]^-$ and $[NTf_2]^-$ anions, while it is smaller than those for ionic liquids with sulfonate anion. Since the betaine dye was unstable in this ionic liquid, we could not determine the value of α.

(52) Marcus, R. A. *J. Phys. Chem.* **1989**, *93*, 3078.

(53) (a) Yonker, C. R.; Frye, S. L.; Kalkwarf, D. R.; Smith, R. D. *J. Phys. Chem.* **1986**, *90*, 3022. (b) Smith, R. D.; Frye, S. L.; Yonker, C. R.; Gale, R. W. *J. Phys. Chem.* **1987**, *91*, 3059.

(54) Maiwald, M.; Schneider, G. M. *Ber. Bunsen-Ges. Phys. Chem.* **1998**, *102*, 960.

(55) McRae, E. G. *J. Phys. Chem.* **1957**, *61*, 562.

(56) Jacquemin, J.; Husson, P.; Padua, A. A. H.; Majer, V. *Green Chem.* **2006**, *8*, 172.

(57) Reynolds, L.; Gardecki, J. A.; Frankland, S. J. V.; Horng, M. L.; Maroncelli, M. *J. Phys. Chem.* **1996**, *100*, 10337.

(58) Horng, M. L.; Gardecki, J. A.; Papazyan, A.; Maroncelli, M. *J. Phys. Chem.* **1995**, *99*, 17311.

(59) (a) Karmakar, R.; Samanta, A. *J. Phys. Chem. A* **2002**, *106*, 6670. (b) Karmakar, R.; Samanta, A. *J. Phys. Chem. A* **2002**, *106*, 4447. (c) Saha, S.; Mandal, P. K.; Samanta, A. *Phys. Chem. Chem. Phys.* **2004**, *6*, 3106. (d) Mandal, P. K.; Sarkar, M.; Samanta, A. *J. Phys. Chem. A* **2004**, *108*, 9048.

(60) Chowdhury, P. K.; Halder, M.; Sanders, L.; Calhoun, T.; Anderson, J. L.; Armstrong, D. W.; Song, X.; Petrich, J. W. *J. Phys. Chem. B* **2004**, *108*, 10245.

(61) (a) Arzhantsev, S.; Ito, N.; Heitz, M.; Maroncelli, M. *Chem. Phys. Lett.* **2003**, *381*, 278. (b) Ito, N.; Arzhantsev, S.; Heitz, M.; Maroncelli, M. *J. Phys. Chem. B* **2004**, *108*, 5771. (c) Ito, N.; Arzhantsev, S.; Maroncelli, M. *Chem. Phys. Lett.* **2004**, *396*, 83. (d) Arzhabtsev, S.; Jin, H.; Ito, N.; Maroncelli, M. *Chem. Phys. Lett.* **2006**, *417*, 524.

(62) Chakrabarty, D.; Hazra, P.; Chakraborty, A.; Seth, D.; Sarkar, N. *Chem. Phys. Lett.* **2003**, *381*, 697.